Supporting information:

A Well-Designed Three-Dimensional Ternary Hierarchical Co-axial ZnO@ZnS Heteroarchitecture Decorated Electrospun Carbon Hollow Tube Nanofibrous Mat: Improved Ultraviolet-Light Photocatalytic Performance

Zahed Shami[1][†]*, Naser Sharifi-Sanjani[1]*

[1]Polymer Laboratory, Chemistry Department, School of Science, University of Tehran, Tehran, Iran.

[†]Pars Petrochemical Company (PPC), Asalouyeh, Boushehr, Iran. www.parspc.net

Corresponding authors

*E-mail: zahed.shami@ut.ac.ir;   z.shami@parspc.net**;**   zahed.shami@gmail.com.   Phone: +989126836425.

*E-mail: nsanjani@khayam.ut.ac.ir. Phone: +982161112488.

1. Experimental Section

Materials. Polyacrylonitrile (PAN, MW = 150 000 g/mol, Polyacryle Co. Esfehan, Iran), paraffin oil (Black Gold Oil, JB, USA), P-25 TiO_2 (Degussa), and ultra pure water, N, N dimethylformamide (DMF), zinc chloride ($ZnCl_2$), methyl orange (MO), thioacetamide (TAA) and ammonia (32%) were all purchased from Merck and used as received.

Preparation of the binary ZnO/C and the ternary coaxial ZnO@ZnS/C hollow tube nanofiber mats. The as-synthesized core-shell carbon hollow nanofiber mats were fabricated by coaxial-electrospinning method, followed by stabilization and finally carbonization, and then combined with a two-steps low temperature hydrothermal process (Figure 1), which consisted of the following steps:

(a) Preparation of the spinnable precursor shell: 0.25 g of zinc chloride was dissolved in 14 mL of DMF with magnetic stirring for 15 min at room temperature and then sonicated (Elmasonic 40 H) for 30 min. Subsequently, 2.5 g of PAN powder was added into the above solution, followed by vigorous stirring for 12 h to obtain a colorless PAN/ZnCl$_2$ shell precursor solution. Paraffin oil was used as the core substance.

(b) Coaxial-electrospinning. The photo image and schematic diagram of the coaxial-electrospinning setup is illustrated in Figure 1. It consists of three major components: a high-voltage power supply, two syringe pumps, and a coaxial spinneret setup. The stainless syringe needles of core (25.0 gauges) and shell (21.0 gauges) constitute the key part of the coaxial spinneret, connected with inner and outer solutions by two Teflon tubes, respectively (inset in Figure 1). The core and shell solutions were delivered independently through the concentric nozzles with the flow rates controlled by two separate syringe pumps. The feeding rates of the outer and inner solutions were 1.2 and 0.07mL/h, respectively. In coaxial-electrospinning process, the collection distance between coaxial spinneret tip and collector was 15 cm and the applied steady-voltage was 14 kV. The obtained shell (PAN/ZnCl$_2$) - core (oil) nanofiber mats were peeled from aluminum foil on a drum collector, plied to form a stable multi-layer mats and then sandwiched between two stainless steel holders with clamps to maintain tension during a high temperature treatment, and dried for 12 h at room temperature under vacuum (Figure S1).

2

(c) Thermal treatment and preparation of ZnO carbon hollow nanofibers (ZnO-C)[1]. In this process, core-shell PAN/ZnCl$_2$ nanofiber mats sandwiched between stainless steel frames were stabilized in a box furnace (Carbolite CWF-1100) with a rising rate of 1°C/ min from room temperature to 290°C in medium atmosphere and kept for 3 h, then they were let to self-cool down to room temperature again, forming stabilized nanofiber mats. Stainless steel sample holders were removed at room temperature. To obtain ZnO carbon hollow nanofiber mats, the stabilized electrospun nano-mats were heated from room temperature to 950°C at 5°C/min in nitrogen atmosphere and kept for 3 h, then they were let to self-cool down to room temperature again (Figure S1). In addition, pure PAN carbon nanofibers were obtained using the same conditions.

(d) Preparation of the binary ZnO decorated onto carbon hollow nanofibrous mats (ZnO/C). ZnO carbon hollow mats were deposited into a solution including 0.54 g of zinc chloride dissolved in 50 mL of distilled water in a Pyrex bottle, forming a clear solution, and the appropriate quantity of ammonia (32%) was added to adjust the pH value to 10.0. The mixed solution was sealed in a bottle and maintained at 90℃ for 4 h in an oven (Binder). Subsequently, the hollow nanofibrous mats coated with ZnO were washed repeatedly with distilled water and ethanol for several times, and then dried in the oven at 60°C for 12 h. The white ZnO powder formed in this process was also collected and dried under the same conditions for comparison.

(e) Preparation of the ternary hierarchical ZnO@ZnS core-shell hetroarchitecture decorated on carbon hollow nanofibrous mats (ZnO@ZnS/C). A 0.25 g TAA were added into a round-bottom flask containing 20 ml of distilled water equipped with a condenser, maintained at 90°C for 9h in an oil bath. The final sample was washed with ethanol and distilled water several times before

3

drying it in a vacuum oven (Binder) at 60°C for 6 h. Furthermore, the synthesized yellow ZnO@ZnS core-shell powder was collected for comparison.

Characterization. The scanning electron microscopy (FE-SEM, Hitachi 54160 and MIRA\\TESCAN-IROST equipped with energy dispersive X-ray detector, EDX), and transmission electronmicroscopy (TEM; Zeiss-EM10C-80KV) were used for morphological characterization of the products. To display the cross- section of the electrospun nanofibrous mats by SEM, the samples were cut with a surgical blade in liquid nitrogen, and then sputtered with a thin gold layer before SEM analysis. Samples for TEM analysis were obtained by two methods. For electrospun PAN/ZnCl$_2$ nanofibers, a 200 mesh carbon grid was attached to the aluminum foil on a drum collector to be coated with a thin nanofiber layer in *in-situ* electrospinning process. In the case of carbon hollow nanofibers, the appropriate quantity of the sample (5 mg) was added to ethanol (2 mL), followed by its sonication for 5 min, and then dropped several times on a carbon grid with a 200 mesh and dried at room temperature. X-ray diffraction (XRD) measurement was carried out using a D/max 2500 XRD spectrometer (Rigaku) with Cu Ka line of 0.15406 nm. Fourier transform infrared (FT-IR) spectra were obtained on Magna 560 FT-IR spectrometer. The photocatalysts photoluminescence (PL) spectra were detected with a JobinYvon HR800 micro-Raman spectrometer using a 325 nm line from a He-Cd laser. UV–Vis absorption spectra (UV–Vis) were performed on a Perkin-Elmer Lambda-25 spectrometer at room temperature.

Photocatalytic degradation test. For practical applicability, the photocatalytic activity of the as-synthesized products was evaluated by monitoring the photo-decolorization of methyl orange (MO) aqueous solution as organic pollutant. 15 mL of an aqueous solution of MO with an initial concentration of 5 ppm was placed in a 50 mL double-walled Pyrex glass reactor with 2.5 cm

inner diameter and 10 cm length under magnetic stirring, cooled by a circulating water bath to maintain the temperature constant and to prevent any evaporation during measurements. The temperature inside the reactor was maintained at about 25°C. A 125 W high pressure mercury vapor UV lamp with a wavelength centered at 365 nm as the irradiation source (Narva NFE 125 W) was positioned at 2 cm above the reactor (Figure S2). The distances between UV irradiation source and MO solution surface and between MO solution surface and bottom of the reactor were 12 cm and 2.7 cm, respectively. The photoreactor was surrounded by a sealed wooden box (40cm∗ 40 cm ∗ 50 cm) equipped with a cooling fan. In order to investigate the photocatalytic performance, the as-obtained product was used as powder and mat. The ternary electrospun mats (10 mg) were tested in two positions: floating and immersed (Figure S2). In the floating position, due to low density and hydrophobic nature, PAN carbon nanofiber mats are suspended on the surface of the solution easily. For immersed position, we used a clip to maintain mats at the bottom of the reactor. For comparison, 10 mg of well powdered ternary ZnO@ZnS/C mats, powder of ZnO@ZnS and pure ZnO were tested as photocatalyst. Furthermore, the commercial P-25 TiO_2 was used as a reference. Prior to irradiation, the all samples were irradiated in the dark for 60 min to reach adsorption/desorption equilibrium between the organic molecule and the surface catalyst. For powdered samples, the suspensions were ultrasound for 5 min in an ultrasonic bath and continuously stirred during the experiments, then collected and centrifuged for 7 min at 4500 rpm (Rotina 380) to separate the photocatalyst particles before measurement. At given irradiation time intervals, 2.0 mL of the sample was removed and MO degradation was studied. Absorbance, an indication of MO concentration, was evaluated by UV−visible spectrophotometer (Perkin-Elmer Lambda-25) monitoring the absorption maximum at $\lambda_{max} = 463$ nm. The percentage of degradation (% D) of MO is reported using following equation:

$$\% \, D = \frac{C_0 - C}{C_0} = \frac{A_0 - A}{A} \times 100$$

where A and C is the absorption and the concentration of pollutant during the reaction, respectively. A_0 and C_0 are its initial absorption and concentration of MO when adsorption–desorption equilibrium was achieved.

2. FT-IR analysis

The chemical composition of as-synthesized samples was analyzed by Fourier transform infrared (FTIR) spectroscopy and indicated in Figure S6. Several well defined bands appeared in the FTIR spectrum. The absence of mainly diffraction peaks reported in PAN nanofibers includes a peak at around 2935 cm^{-1} assigned to the stretching vibration of the methylene (–CH$_2$–) group, a peak at around 2240 cm^{-1} due to the stretching vibration of nitrile groups (–CN–) and a peak at about 1450 cm^{-1} for the bending vibration of methylene (–CH$_2$–) support carbonized PAN nanofibers[2]. The well-defined band in pure carbon hollow nanofibers at 1612 cm^{-1} corresponds to C=C stretching vibrations, confirming the thermal cyclization process. The broad absorption peak at about 3438-3410 cm^{-1} and a peak at 1612-1602 cm^{-1} may be attributed to O–H stretching vibration and H–O–H bending vibration of chemisorbed and/or physisorbed H$_2$O molecules, respectively[3,4]. These peaks are more pronounced for ZnO/C and ZnO@ZnS/C heterostructures. The further adsorbed H$_2$O molecules confirm increase in the surface area provided by formation of nano-heterostructures. The absorption band situated at about 2366 cm^{-1} is suggested to be attributed to the vibration of carbon dioxide adsorbed from the atmosphere[5]. Generally, the FT-IR spectra recorded in the spectral range of around 500 cm^{-1} indicate metal lattice vibration modes[6-10]. The origination of a well-defined band at 456 cm^{-1} is due to metal-oxygen (Zn-O-Zn)

mode and hence confirms the formation of ZnO nanoparticles. It is observed that the diffraction peak located at about 456 cm^{-1} present in the FT-IR spectrum of ZnO/C hollow nanofibers is split into two peaks, one very weak peak at around 451cm^{-1} assigned to ZnO vibration and the other strong peak situated at about 482 cm^{-1} attributed to the Zn-S-Zn vibration in ZnS crystal[11,12], verify ZnO particles coated with ZnS layer, as shown in TEM and FE-SEM images.

3. Figure captions

Figure S1. Heat treatment procedure photographs of co-axial electrospinning nanofibrous mats.

Figure S2. Schematic representation of photocatalytic analysis of the ternary ZnO@ZnS/C hollow tube nanofibrous (a) floating, (b) immersed and, (c) powdered mat.

Figure S3. TEM image of PAN/ZnCl$_2$ core-shell nanofibers reveals ZnCl$_2$ particles distribution on the outer surface nanofibers.

Figure S4. Additional FE-SEM images of the as-synthesized electrospun ZnO@ZnS/C hollow tube nanofibers in different magnifications.

Figure S5. Additional TEM image of the as-synthesized electrospun ZnO@ZnS/C hollow tube nanofibers.
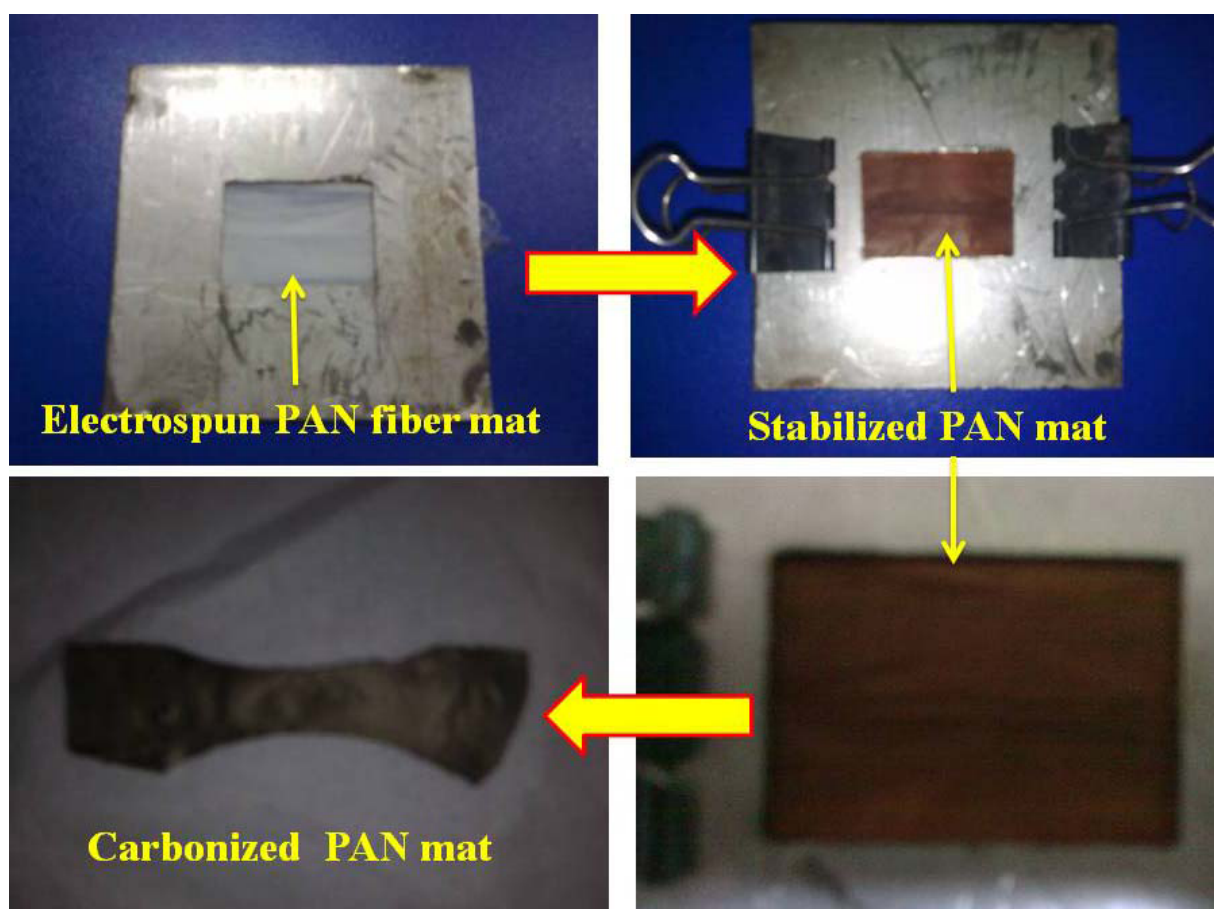
Figure S6. FT-IR reflectance spectra of the as-synthesized electrospun hollow tube nanofibrous mats.
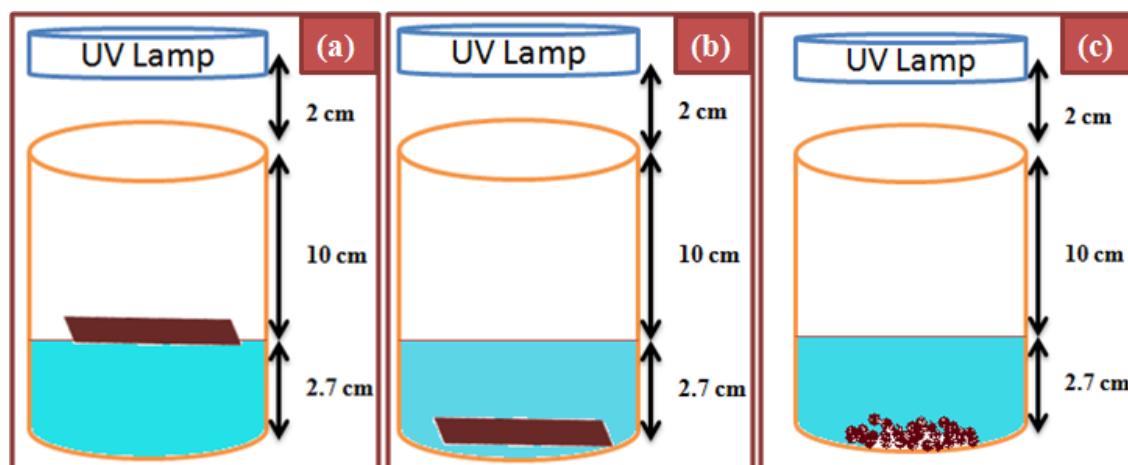
References

1.   L. Ji, Fiber and Polymer Science, 2009.

2.   I. H. Chen, C.-C. Wang and C.-Y. Chen, *Carbon*, 2010, **48**, 604-611.

3.   H. Yu, H. Zhang, H. Huang, Y. Liu, H. Li, H. Ming and Z. Kang, *New Journal of Chemistry*, 2012, **36**, 1031-1035.

4.   F. Davar, M. Mohammadikish, M. Reza Loghman-Estarki and Z. Hamidi, *CrystEngComm*, 2012, **14**, 7338-7344.

5.   P. Galhotra, Graduate College ,The University of Iowa, 2010.

6.   D. Wu, Y. Jiang, Y. Yuan, J. Wu and K. Jiang, *J Nanopart Res*, 2011, **13**, 2875-2886.

7.   M. T. Uddin, Y. Nicolas, C. Olivier, T. Toupance, L. Servant, M. M. Müller, H.-J. Kleebe, J. Ziegler and W. Jaegermann, *Inorganic Chemistry*, 2012, **51**, 7764-7773.

8.   J. Mu, C. Shao, Z. Guo, Z. Zhang, M. Zhang, P. Zhang, B. Chen and Y. Liu, *ACS Applied Materials & Interfaces*, 2011, **3**, 590-596.

9.   R. Kumar, G. Kumar and A. Umar, *Materials Letters*, 2013, **97**, 100-103.

10.   S. Sarkar, A. Makhal, T. Bora, K. Lakhsman, A. Singha, J. Dutta and S. K. Pal, *ACS Applied Materials & Interfaces*, 2012, **4**, 7027-7035.

11.   S. Muthukumaran and M. Ashok kumar, *Materials Letters*, 2013, **93**, 223-225.

12.   L. Wang, S. Huang and Y. Sun, *Applied Surface Science*, 2013, **270**, 178-183.
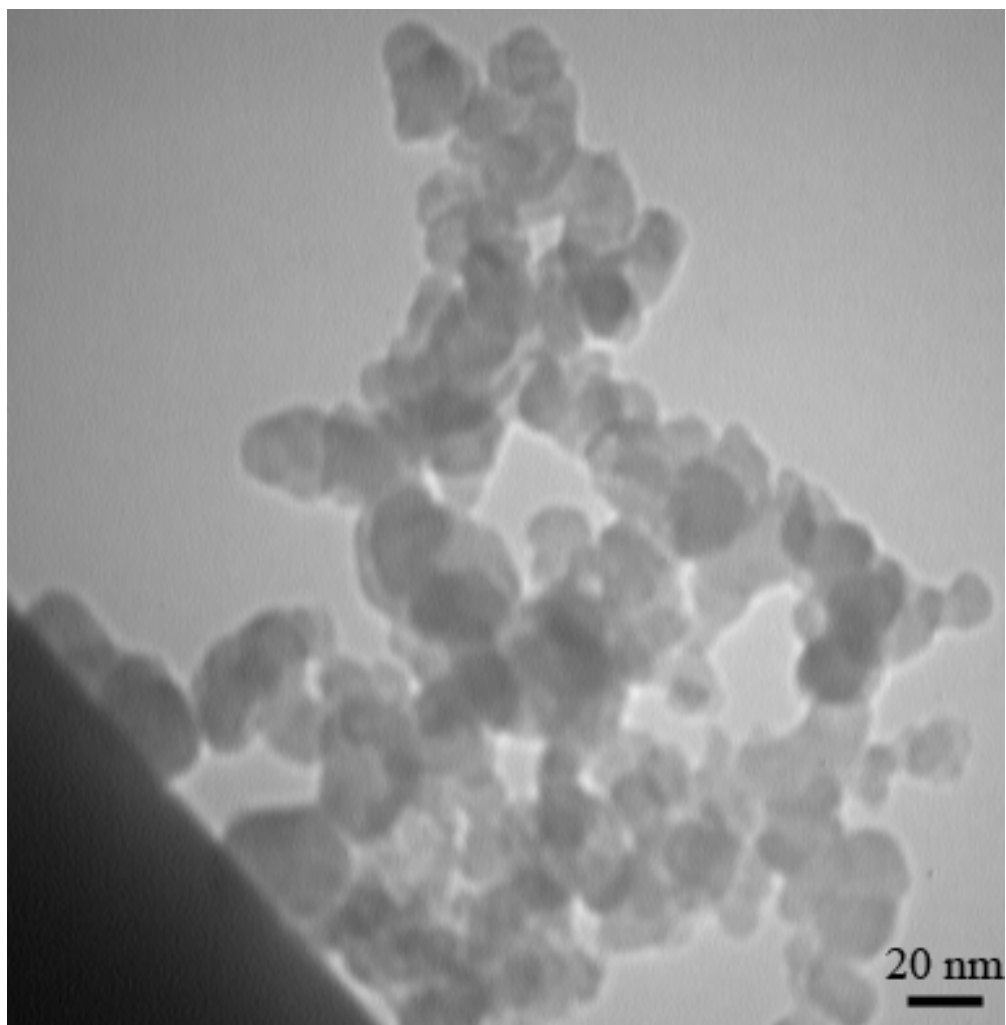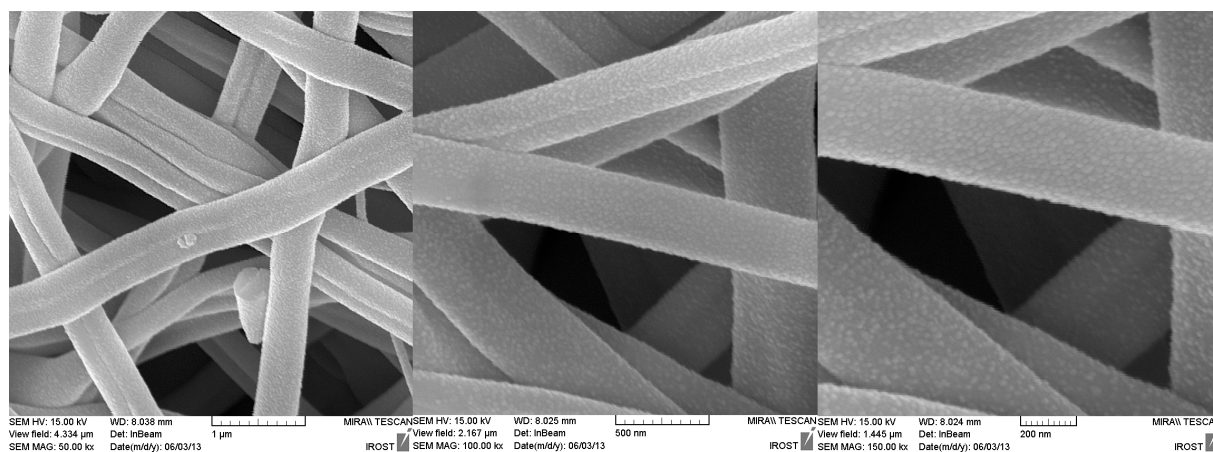
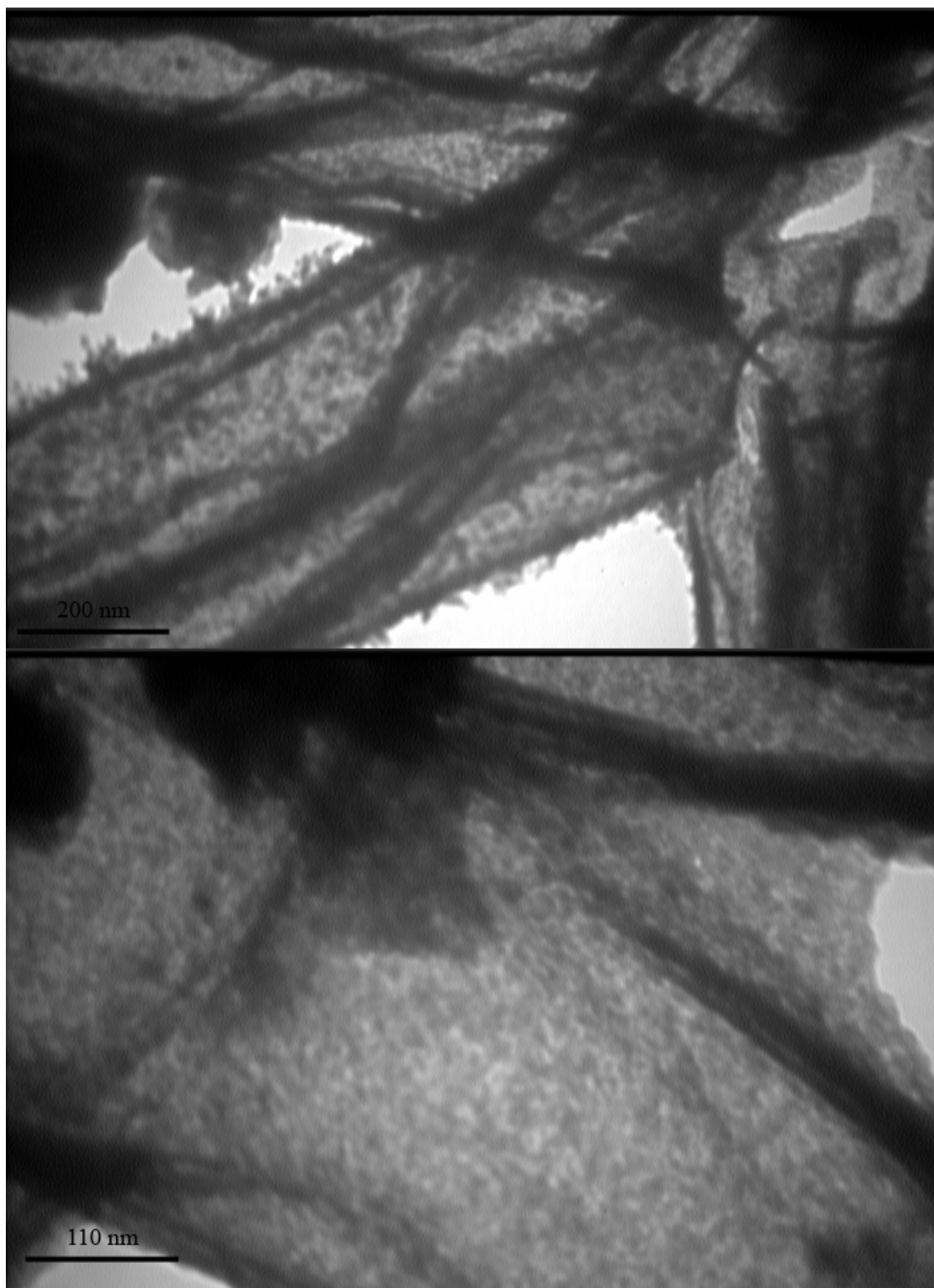**Figure S1.** Heat treatment procedure photographs of co-axial electrospinning nanofibrous mats.

Figure S2. Schematic representation of photocatalytic analysis of the ternary ZnO@ZnS/C

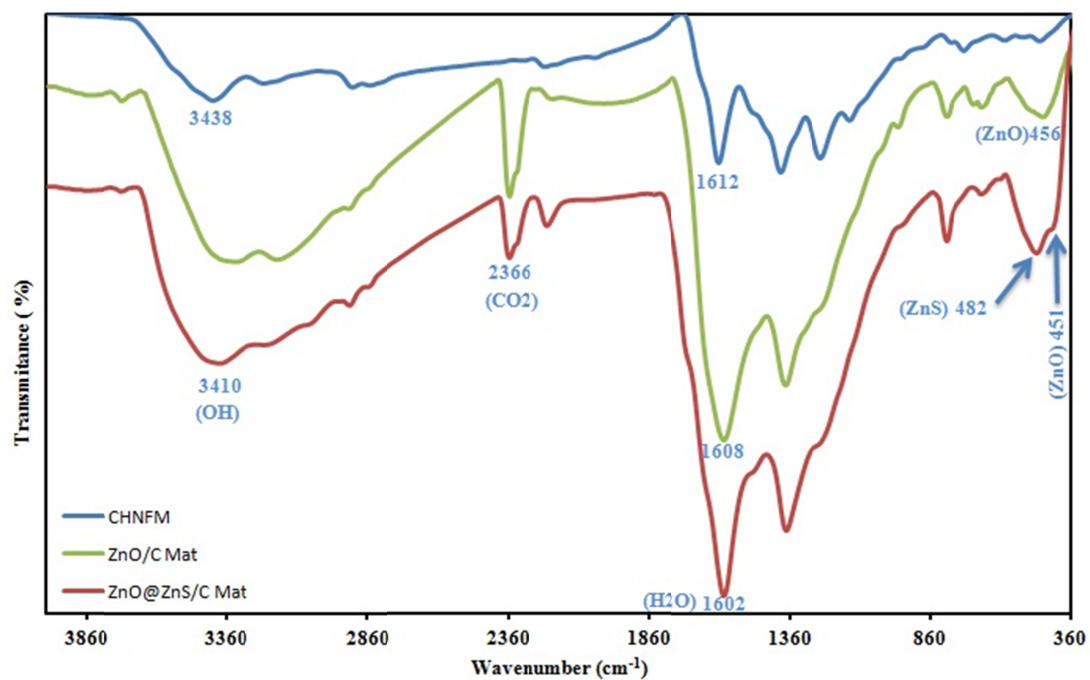hollow tube nanofibrous (a) floating, (b) immersed and, (c) powdered mat.

Figure S3. TEM image of PAN/ZnCl$_2$ core-shell nanofibers reveals ZnCl$_2$ particles distribution

on the outer surface nanofibers.

SEM HV: 15.00 kV	WD: 8.038 mm		1 µm	MIRA\\ TESCAN	SEM HV: 15.00 kV	WD: 8.025 mm		500 nm	MIRA\\ TESCAN	SEM HV: 15.00 kV	WD: 8.024 mm		200 nm	MIRA\\ TESCAN
View field: 4.334 µm	Det: InBeam				View field: 2.167 µm	Det: InBeam				View field: 1.445 µm	Det: InBeam			
SEM MAG: 50.00 kx	Date(m/d/y): 06/03/13			IROST	SEM MAG: 100.00 kx	Date(m/d/y): 06/03/13			IROST	SEM MAG: 150.00 kx	Date(m/d/y): 06/03/13			IROST

Figure S4. Additional FE-SEM images of the as-synthesized electrospun ZnO@ZnS/C hollow tube nanofibers in different magnifications.

12

Figure S5. Additional TEM image of the as-synthesized electrospun ZnO@ZnS/C hollow tube nanofibers.

Figure S6. FT-IR reflectance spectra of the as-synthesized electrospun hollow tube nanofibrous mats.